

THE USE OF HORIZONTAL AXIS COILS FOR THE EDDY CURRENT  
INSPECTION OF FAST BREEDER REACTOR PRIMARY VESSELS

R. Clark, L. J. Bond and P. French  
Non-Destructive Evaluation Centre  
Department of Mechanical Engineering  
University College London  
Torington Place  
London WC1E 7 JE UK

INTRODUCTION

The inspection of nuclear power plant is one of the most demanding fields in which non-destructive evaluation (NDE) is required to be performed. In Europe, the proposed next generation of nuclear reactors are liquid metal cooled fast breeder reactors (LMFBR). This paper reports on an investigation into the feasibility of using eddy current techniques for inspecting the primary austenitic vessel of the LMFBR.

The use of horizontal axis coils in this study was prompted by the work of Riaziat and Auld [1] who have suggested that horizontal axis coils may be better for flaw detection than the more conventional vertical axis coils.

An analytical theory (due to Burke [2]) has been used to obtain impedance change values when a horizontal axis coil is brought close to a conducting half space. These values have been compared with experimental data and with values obtained from a newly developed approximate model for the half space system. The approximate model assumes that the inducing magnetic field is uniform in the surface of the material half space. The approximate model has been extended to consider half space stratification.

ANALYTICAL THEORY

Burke [2] has put forward two analytical expressions which can be used to calculate the impedance change of a horizontal axis coil as it is brought close to a homogeneous conducting half space. One expression is a perturbation expansion which is valid for small skin depth,  $\delta$ , values and the other is an exact solution which is valid for all values of  $\delta$ .

The perturbation expansion expression has the form

$$\Delta Z = -2i\omega\mu_0 \left( \frac{N}{t(a_2 - a_1)} \right)^2 \times \int_0^{\infty} \frac{ds}{s^6} \sin^2(st) M^2(sa_1, sa_2) R(sd) \quad (1)$$

where  $N$  is the number of coil turns,  $t$  is the coil half length,  $a_1$  is the coil inner radius,  $a_2$  is the coil outer radius,  $d$  is the distance from coil axis to material surface, and

$$M(sa_1, sa_2) = \int_{sa_1}^{sa_2} d(sa) sa I_1(sa)$$

$$R(sd) = K_0(2sd) + (i-1)s\delta\mu_r K_1(2sd) + \dots$$

The exact solution has the form

$$\Delta Z = -2i\omega\mu_0 \left( \frac{N}{t(a_2 - a_1)} \right)^2 \int_0^\infty \frac{ds}{s^6} M^2(sa_1, sa_2) \sin^2(st) \times \int_0^\infty dp \frac{(\mu_r \alpha - \alpha_1)}{\alpha(\mu_r \alpha + \alpha_1)} \exp(-2\alpha d) \quad (2)$$

where  $\alpha = (p^2 + s^2)^{1/2}$ ,  $\alpha_1 = (\alpha^2 + i\omega\sigma\mu_r)^{1/2}$  and the other terms are as defined for (1). Both of these expressions were coded for evaluation on a computer. To confirm the accuracy of these programs, results were produced using Burke's coil and material data. The program results are compared with Burke's results in Fig 1. Both of the programs written produced results which verified Burke's plots. The differences were due to the different methods of computation used.

#### APPROXIMATE MODEL

The approximate theory for the eddy currents in a stratified half space is outlined briefly here. A more detailed description is given elsewhere [3].

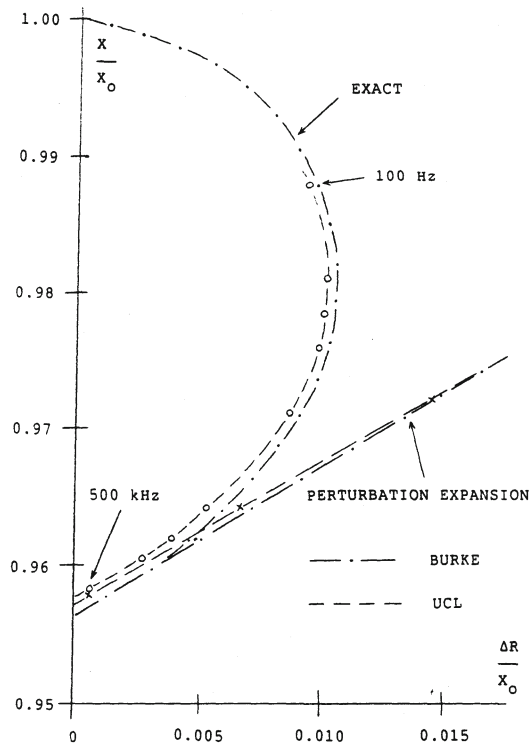


FIG 1. Comparison of results produced by Burke and UCL for the analytical theory of Burke [2]

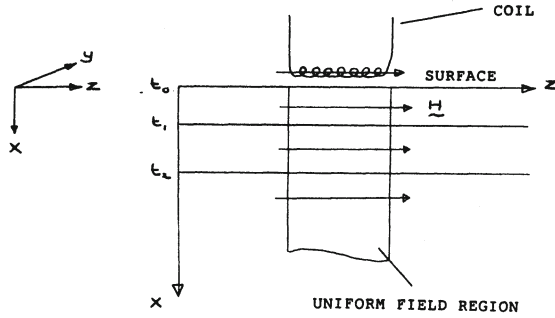


FIG 2. Geometry for approximate model

Using Maxwell's electromagnetic field equations as a base, Libby [4] has shown that a partial differential equation pair can be obtained, one in terms of  $E$ , the electric field intensity, and one in terms of  $H$ , the magnetic field intensity, which describe the electromagnetic field in an infinite, homogeneous and isotropic conducting media. The  $H$  equation has been used as the basis of the new model. In order to keep the model simple the form of the  $H$  field was chosen to be

$$\underline{H} = \begin{pmatrix} 0 \\ 0 \\ \underline{H}(x) \end{pmatrix} \quad (3)$$

given the co-ordinate system in Fig 2. The only variation in the field is a change in the magnitude with increasing depth into the material. Since the field is assumed to vary sinusoidally with time, the partial differential equation for  $H$  can be written as an ordinary differential equation in the form

$$\frac{d^2 \underline{H}}{dx^2} = k^2 \underline{H} \quad (4)$$

where  $k^2 = i \omega \sigma \mu$ . A similar equation can be found for  $E$ . The general solutions for the equations are

$$H_i = A_i e^{+k_i x} + B_i e^{-k_i x} \quad (5)$$

and

$$E_i = - \left( \frac{k_i}{\sigma_i} \right) \left[ A_i e^{+k_i x} - B_i e^{-k_i x} \right] \quad (6)$$

where  $i$  denotes the layer in a layered half space and  $A$  and  $B$  are coefficients that need to be evaluated. To evaluate the coefficients  $A$  and  $B$ , the problem boundary conditions need to be applied. There are three sets of boundary conditions,

$$1) \quad \text{at } x = 0 \quad H = H_0 \quad \text{and} \quad E = E_0 \quad (7)$$

( $H_0$  and  $E_0$  are the surface field values)

$$2) \quad \text{at } t = t_n \quad H_{t_n^-} = H_{t_n^+} \quad \text{and} \quad E_{t_n^-} = E_{t_n^+} \quad (8)$$

(the tangential components of the  $\underline{H}$  and  $\underline{E}$  fields are continuous at the layer interfaces)

$$3) \text{ as } x \rightarrow \infty, H \text{ and } E \rightarrow 0 \quad (9)$$

An approach based on the theory of Brick and Snyder [5] has been used to determine the field outside a finite length solenoid. Assuming magnetostatic conditions, the expression for H in the z-direction outside the coil and at large radial distances from the coil is

$$H = \left( \frac{n I a^2}{2l^2} \right) \left( 1 + \frac{r^2}{l^2} \right)^{-3/2} \quad (10)$$

where n is the number of turns/metre, a is the coil radius, r is the radial distance from z-axis to external point, I is the current through each turn, and 2l is the length of coil.

A point was considered at a large radial distance from the coil. At this point it was assumed that the field (H) value had decreased to 0.1% of the value of H on the central axis of the solenoid. Using (10) the value of r at this point was determined. This value of r was then referred to as  $r_\infty$ , the point at which the field could be considered to have decreased to zero. It was assumed that the field decayed from the coil axis to  $r_\infty$ . The decay mode was taken to be of the form 1/r, as indicated by the Biot Savart law. Hence

$$H = \left( \frac{1}{r} - \frac{1}{r_\infty} \right) H_c \quad (11)$$

where  $H_c = H$  on the central axis of the solenoid. This enabled the determination of the value of H at the surface of the conducting half space beneath the coil. H can be related to the changes in resistance and inductance of the measuring coil due to the presence of the conducting half space by considering (12) and (13).

$$\Delta R = \frac{1}{\sigma I^2} \int_{\text{vol}} \frac{dH}{dx} \cdot \frac{dH^*}{dx} dv \quad (12)$$

where  $\Delta R$  is the change in resistance and I is the peak current.

$$\Delta L = \frac{\mu}{I^2} \int_{\text{vol}} \underline{H} \cdot \underline{H}^* dv \quad (13)$$

where  $\Delta L$  is the change in inductance.

It also needs to be stated that

$$R_{\text{coil}} = R_0 + \Delta R \quad (14) \quad \text{and} \quad L_{\text{coil}} = L_0 - \Delta L \quad (15)$$

where  $R_{\text{coil}}$  is the coil resistance in the presence of the half space, and  $R_0$  is the coil resistance in air.

The problem encountered with this approach was that the two H fields in equations (12) and (13) were different. The primary magnetic field is responsible for the eddy current induction and is the H field in equation (12). The secondary flux field which leads to a reduction in the coil inductance is the  $\underline{H}$  field in equation (13).

The surface value of H for the secondary field needs to be

determined such that the equations can be evaluated. A simple expression for the secondary surface H value has been put forward. Since the only variable between the tests on a certain piece of material was the frequency, the expression proposed was

$$H_{so} = H_{po} \sqrt{\frac{f}{f_{co}}} \quad (16)$$

where  $f$  is the frequency,  $f_{co}$  is the crossover frequency (the frequency value at which the experimental and approximate  $\Delta L$  plots cross when  $H_{po}$  is used in the calculation),  $H_{so}$  is the secondary surface H value, and  $H_{po}$  is the primary surface H value.

The expression produced reasonably good results over the frequency range considered. The value of  $f_{co}$  was material dependent.

Field uniformity was needed for the model to be valid. Directly underneath the test coil this was the case (Fig 2), hence the volume over which the integrations were performed was taken to be

$$dv = 2l \cdot 2a \cdot dx \quad (17)$$

#### EXPERIMENTAL WORK

A simple experimental configuration was used. Two coils were wound on separate perspex rod formers using coated copper wire to form a single layer.

<u>Coil 1</u>	<u>Coil 2</u>
140 turns	200 turns
Rod Diameter = 10 mm	Rod Diameter = 10 mm
Coil Length = 39 mm	Coil Length = 29 mm
Wire Diameter = 0.25 mm	Wire Diameter = 0.122 mm

Each coil was connected to a Wayne Kerr 6425 microprocessor based precision component analyser. The analyser provided a direct readout of the impedance of the component connected between the two output terminals of the instrument.

The metal specimens used were a block of 316 stainless steel and a sheet of copper. A layered specimen was also considered, it consisted of 1.62 mm of copper on a stainless steel block.

The test procedure involved bringing a coil close to the specimen at several frequencies in the range 100Hz to 100kHz. A lift-off of 0.143 mm was maintained throughout. The values for the change in resistance and the change in inductance of the coil were recorded.

#### RESULTS AND DISCUSSION

Several test cases have been considered using both computer models and by performing some simple experiments. The results presented have been chosen to demonstrate the use of two different coils, the effect of variations in lift-off and the study of a layered specimen.

Figs 3a and 3b illustrate the resistance and inductance characteristics when the 140 turn coil is brought close to a 316 stainless steel block. The trends demonstrated are as expected,  $\Delta R$  becomes more positive with increased frequency and  $\Delta L$  becomes more negative with increased frequency. The approximate model and experiment

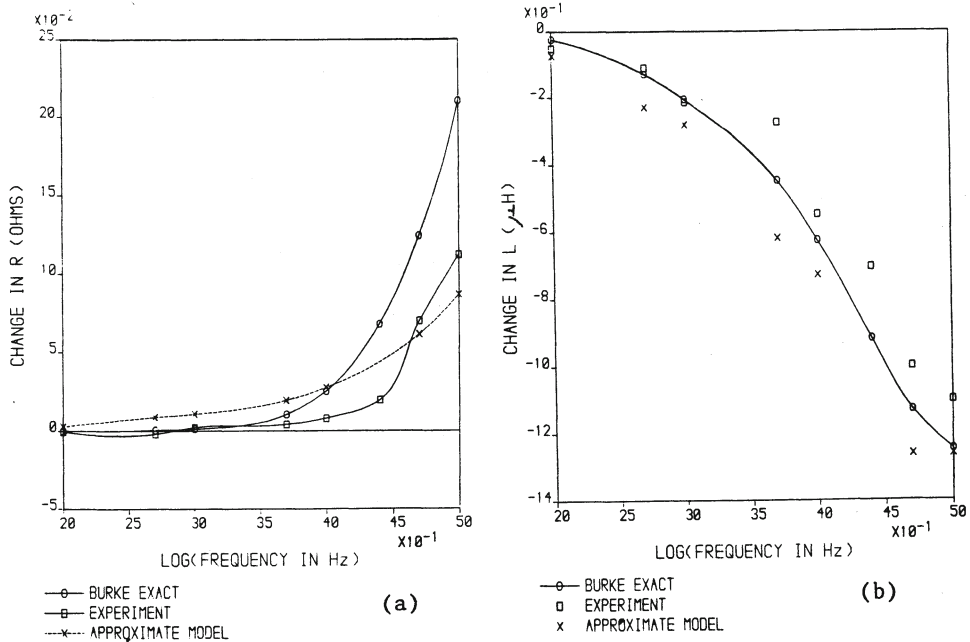


FIG 3. 140 turn coil above 316 stainless steel (a)  $\Delta R$  v log (frequency) (b)  $\Delta L$  v log (frequency)

agree quite well over the range of frequency considered, although the two plots do start to diverge at high frequency (100kHz). At high frequencies the skin effect phenomenon in the coil wire becomes significant [6]. This was not considered in the approximate model and would thus account for some of the model underestimation of the  $\Delta R$  value. The results obtained from the Burke exact solution were an overestimation

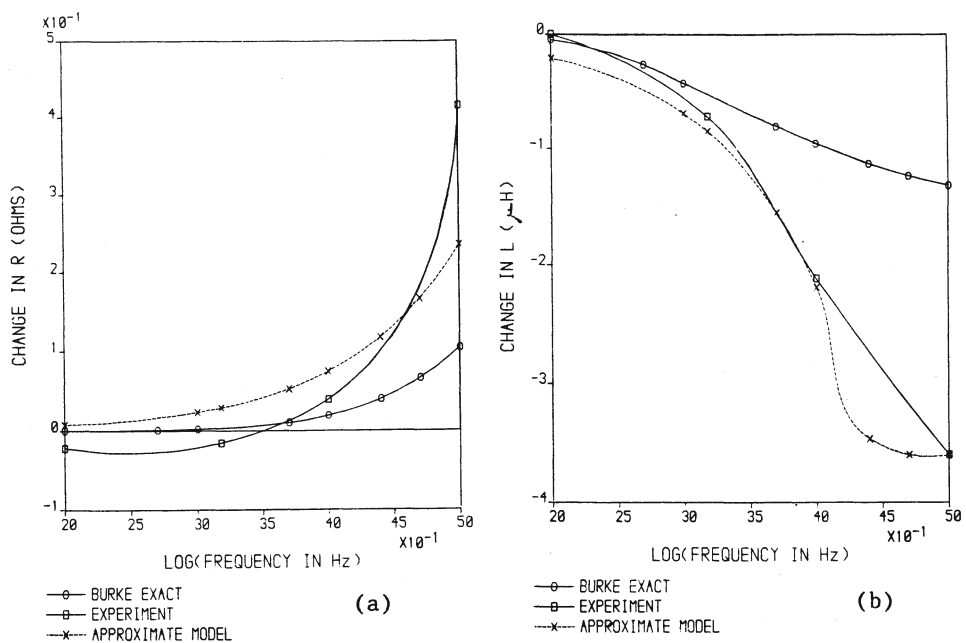


FIG 4. 200 turn coil above 316 stainless steel (a)  $\Delta R$  v log (frequency) (b)  $\Delta L$  v log (frequency)

of the experimental  $\Delta R$  values at high frequencies. The reason for the difference was attributed to errors with the exact solution computation. It must be noted that the experimental results obtained for frequencies below 1.5kHz were subject to large possible errors ( $\Delta R \pm 105\%$ ,  $\Delta L \pm 41\%$ ). The  $\Delta L$  results (Fig 3b) show good agreement across the entire frequency range considered. The results produced by the approximate model theory compare well, thus indicating the usefulness of the simple expression developed.

Figs 4a and 4b illustrate the results for the 200 turn coil when it is brought close to a 316 stainless steel block. The results compare well below 10kHz, but above this frequency the agreement is less definite. This was especially true when considering the Burke exact data. The differences were attributed to computational errors and experimental errors.

Using the 140 turn coil above the 316 stainless steel block, an investigation of the effect of lift-off variation was performed (Fig 5). These results indicate that although the horizontal coil is sensitive to lift-off, the impedance changes associated with varying degrees of lift-off are small compared to those obtained with a vertical axis coil in the same situation. It must be stated that the signals obtained from horizontal coils are in general smaller ( $m\Omega$  and  $\mu H$ ) than those obtained from vertical axis coils ( $\Omega$  and  $mH$ ).

In order to demonstrate the use of the approximate model for the consideration of a stratified half space, Figs 6a and 6b have been included. Here a 1.62 mm thick layer of copper on a 316 stainless steel block has been investigated. The trends exhibited by the model results provide a useful approximation to the experimental values of  $\Delta R$  and  $\Delta L$ .

The results presented illustrate some of the work performed during the initial evaluation of the use of horizontal coils for eddy current inspection. Much of the data has been presented in the form of plots of  $\Delta R$  and  $\Delta L$  versus frequency. This was done in order to make the results clearer and easier to understand. The assumptions included in the

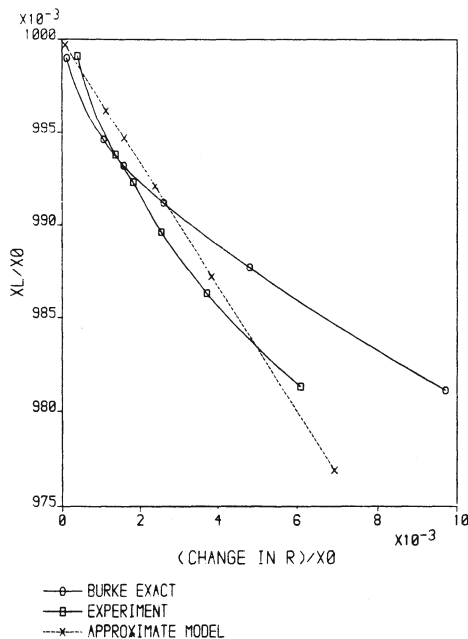


FIG 5. Lift-off variation - 140 turn coil above 316 stainless steel

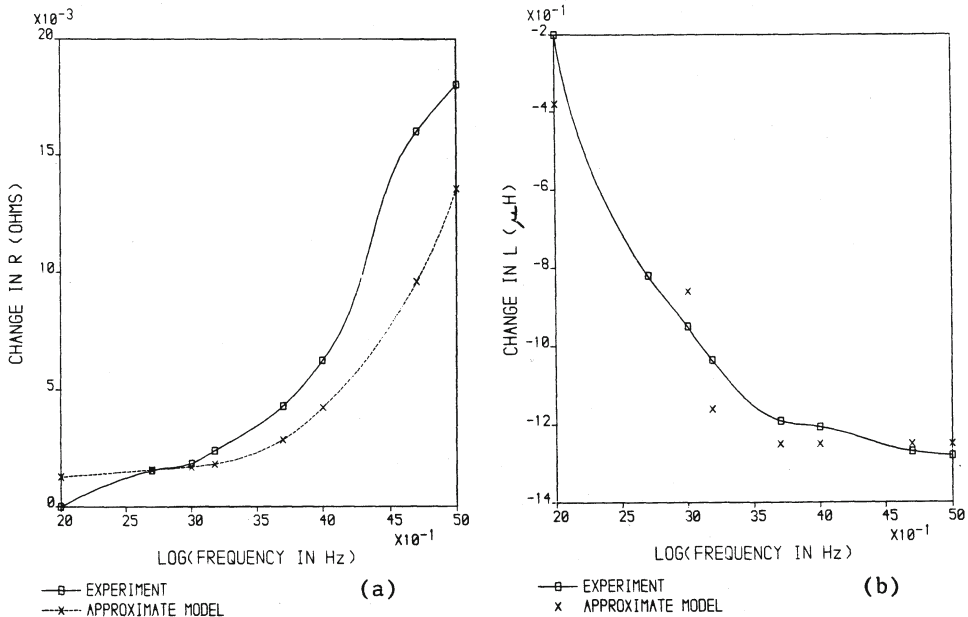


FIG 6. 140 turn coil above 162mm of copper on 316 stainless steel (a)  $\Delta R$  v log (frequency) (b)  $\Delta L$  v log (frequency)

approximate model had an effect on the accuracy of the model, but the work has demonstrated that given the ease of programming and the speed of calculation relative to the Burke theory, the approximate model offers a useful first approximation for the values of  $\Delta R$  and  $\Delta L$ .

#### CONCLUSIONS

This paper has described the initial phase of work that has considered the use of horizontal axis coils for eddy current inspection of austenitic pressure vessels. The initial results look promising, the experimental values comparing well with those obtained from two completely different theoretical models for the case of a coil above a conducting half space. Although the approximate model does not have the accuracy of the more rigorous analytical theory, it does have the advantages of being easily programmable and quick to use.

#### ACKNOWLEDGEMENT

This work has been supported by the Science and Engineering Research Council and the Northern Research Laboratories of the United Kingdom Atomic Energy Authority at Risley, Cheshire, UK.

#### REFERENCES

- 1 M. Riaziat and B. A. Auld, in Review of Progress in QNDE, edited by D. O. Thompson and D. E. Chimenti (Plenum Press, New York, 1984), Vol. 3A, pp. 511-521.
- 2 S. K. Burke, J. Phys. D **19**, 1159-1173 (1986).
- 3 R. Clark, L. J. Bond and P. French, paper in preparation (1988).
- 4 H. L. Libby, Introduction to electromagnetic NDT methods (Wiley-Interscience, 1971).
- 5 D. B. Brick and A. W. Snyder, Amer. J. Phys. **33**, 905-909 (1965).
- 6 F. E. Terman, Radio Engineering, 3rd ed. (McGraw Hill, 1951).